MOVING VEHICLE DETECTION USING A SINGLE SET OF QUICKBIRD IMAGERY — AN INITIAL STUDY

Yun Zhang and Zhen Xiong

Department of Geodesy and Geomatics Engineering, University of New Brunswick
15 Dineen Dr., P.O. Box 4400, Fredericton, New Brunswick, Canada E3B 5A3 - (YunZhang, zxiong)@unb.ca

Commission VII

KEY WORDS: Moving vehicle, high resolution, satellite imagery, single set imagery

ABSTRACT:

Moving vehicle detection has become increasingly important in transportation management and road infrastructure development. State-of-the-art moving vehicle detection techniques require multi-frame images or at least a stereo pair of aerial photos for moving information extraction. This paper presents a new technique to detect moving vehicles using just one single set of QuickBird imagery, instead of using airborne multi-frame or stereo images. To find out the moving information of a vehicle, we utilize the unnoticeable time delay between multspectral and panchromatic bands of the QuickBird (or Ikonos) imagery. To achieve an acceptable accuracy of speed and location information, we first employ a refined satellite geometric sensor model to precisely register QuickBird multispectral and panchromatic bands, and then use a new mathematic model developed in our research to precisely calculate the ground position and moving speed of vehicles detected in the image. The initial testing results demonstrate that the technique developed in this research can extract information on position, speed, and moving direction of a vehicle at a reasonable accuracy.

1. INTRODUCTION

For developing an efficient, safe, environmental sustainable, mobile and accessible transportation infrastructure, timely and continuously distributed traffic information for a large coverage of the regions of interest has become increasingly important. The typical traffic parameters for developing or improving an effective transportation system include vehicle presence, count, speed, class, gap, headway, etc. (STDI and U.S. Department of Transportation, 2000).

To collect traffic information, on-ground monitoring or measurement is still the main stream. Recent research reports are, for example, ground laser or video techniques for highway traffic monitoring (e.g.,Yamada and Soga, 2003), on-ground sensing devises for moving target detection (e.g., Yamada and Soga, 2003; Sun, *et al*., 2005), and no-ground radar measurements (Nag, 2003). All these techniques can only collect traffic information at certain locations where the devices are located.

Only a few research reports or proposals have introduced techniques of using airborne optical or satellite SAR sensors for moving vehicle or target detection**.** Two types of technologies have been found in our literature review:

(1) Using synthetic aperture radar (SAR) for moving target detection, which is carried out in two different ways: (a) virtually partitioning a large radar antenna into two sub-apertures to receive two returns from a target at different times (e.g., Defence R&D Canada, 2004); (b) utilizing the motion and time delay of a SAR sensor to detect moving targets according to multiple signals received from a target (e.g., Dias and Marques, 2005).

(2) Using multi-frame airborne images taken by a video, two still cameras or other devices to find moving information (e.g., Zhang and Chen. 2005, Rad and Jamzad, 2005).

These techniques have the potential to provide large coverage, continuously distributed traffic information. However, they still face technical challenges for an automated operation.

None publications have been found which use optical satellite imagery for moving vehicle detection, especially using a single set of optical imagery. To detect moving vehicles, two major challenges have to be overcome: (1) detection of vehicles in the imagery, and (2) calculation of the location, speed and moving direction of the vehicles. The solutions for problems in the second challenge are not straightforward when stereo image pairs are used. They are much more difficult when a single set of QuickBird or Ikonos image data is employed.

To solve the problems in calculating location, speed and moving direction of detected vehicles, we present a novel technique to detect moving speed of vehicles using just a single set of high resolution satellite imagery. The novelty of this technique is not just the use of optical satellite imagery for moving vehicle detection, but more important is the use of only one single set of imagery for speed measurement, instead of using multi-frame or stereo images.

To find out the moving information of a vehicle, we utilize the unnoticeable time delay between multspectral (MS) and panchromatic (Pan) bands of the QuickBird (or Ikonos) imagery. To achieve an acceptable accuracy of speed and location information, we first employ a refined satellite geometric sensor model to precisely register QuickBird MS and Pan bands, and then use a new mathematic model developed in this research to precisely calculate the ground position and moving speed of the vehicles. The initial testing results demonstrate that the technique developed in this research can obtain information on position, speed, and moving direction of a vehicle at a reasonable accuracy.

2. METHODOLOGY

2.1 Fundamental rationale

Most of the latest high resolution satellites, such as QuickBird and Ikonos, capture both panchromatic (Pan) and multispectral (MS) images simultaneously. But the Pan and MS images are not exactly taken at the same time due to the arrangement of CCD (Charge Coupled Device) arrays. There is an unnoticeable viewing angle difference between the Pan and MS arrays causing a very little time interval between the Pan and MS images. Therefore, if a ground vehicle is moving, the vehicle should theoretically be imaged in different ground positions on the Pan and MS images, even though the difference id very small. If we can precisely calculate the ground position of the vehicle from the Pan and MS images, we should be able to obtain two different ground coordinates for the same vehicle. We can then determine the moving speed and moving direction of the vehicle. This is the fundamental rationale of our moving vehicle detection technique.

However, because the time interval between the Pan and MS images is very little, less than 1 second, the position change of a moving vehicle is also very small.

So if the error of position calculation is greater than the size of its position change, we can never detect moving vehicle correctly. Therefore, some methods must be used to minimize the errors of vehicle position calculation. Besides, because we generally use satellite geometric sensor model to calculate the vehicle ground position, so the accuracy of object ground position is directly related with the satellite geometric sensor model. Therefore how to refine the satellite sensor model to improve vehicle position accuracy is also our focus.

2.2 Satellite geometric sensor model refinement

2.2.1 Problems with original sensor models: Different satellite has different physical geometric sensor model with different positioning accuracy. To date, some satellite image vendors, such as SPOT, directly provide users with a physical sensor model. But some others do not, such as IKONOS and Qucikbird, because of technical confidentialities. In stead of physical sensor models, these satellite image vendors just release a set of rational polynomial coefficients (RPCs) and use a set of rational polynomial functions (RPFs, Equation 1) to model their sensor geometry.

$$\begin{cases} x = \dfrac{P_1(X,Y,Z)}{P_2(X,Y,Z)} & \text{(1a)} \\ y = \dfrac{P_3(X,Y,Z)}{P_4(X,Y,Z)} & \text{(1b)} \\ P(X,Y,Z) = \sum_{i=0}^{m1}\sum_{j=0}^{m2}\sum_{k=0}^{m3} a_{ijk} X^i Y^j Z^k & \text{(1c)} \\ 0 \le m_1 \le 3, \\ 0 \le m_2 \le 3, \\ 0 \le m_3 \le 3,\ m_1 + m_2 + m_3 \le 3 & \text{(1d)} \end{cases}$$

Where (x, y) is the image coordinates and (X, Y, Z) is the ground coordinates, a_{ijk} is the polynomial coefficients (RPCs).

No matter what sensor models are provided, direct physical sensor models or RPCs, all of them usually contain a definite value of absolute positioning errors. For example, according to our experiments, the SPOT 1, 2, 4 has an absolute positioning error of around 300 meters and the SPOT 5 has an absolute positioning error of about 50 meters, before the sensor models are refined with certain ground control points (GCPs). IKONOS and Quickbird usually have an absolute positioning error of about 20 meters. Therefore, if original models are directly employed to calculate object ground position, the sensor model error will be propagated to the ground position of the vehicles. The position error of a vehicle may be greater than the moving distance of a vehicle during the tiny time interval between Pan and MS. The result of speed calculation will then be ridiculous. Sometimes the speed detection result may show that a static vehicle is moving while a moving vehicle is static. Consequentially, a significant improvement of the sensor model accuracy is crucial for detecting moving vehicles and calculating the speed of a moving vehicle.

2.2.2 Existing sensor model refinement: Many research publications have reported different ways to improve the geometric accuracy of different sensor models. Di *et al*. (2003) recognized that there are two methods to improve the geopositioning accuracy of Ikonos Geo products.

- The first is to compute a set of new rational polynomial coefficients (RPCs), in which the vender-provided RPCs were used as initial values for Equations 1, and a large number of GCPs was then required to compute the new RPCs. For a set of third-order rational coefficients, more than 39 GCPs are required.
- The second method was to improve the ground coordinates derived from Equation 1 using the vendor-provided RPCs. A polynomial correction (Equation 2) was applied to the correction of the ground coordinates, in which the parameters (correction coefficients) are determined by the GCPs.

$$\begin{cases} X = a_0 + a_1 X_{RF} + a_2 Y_{RF} + a_3 Z_{RF} & \text{(2a)} \\ Y = b_0 + b_1 X_{RF} + b_2 Y_{RF} + b_3 Z_{RF} & \text{(2b)} \\ Z = c_0 + c_1 X_{RF} + c_2 Y_{RF} + c_3 Z_{RF} & \text{(2c)} \end{cases}$$

Where (X, Y, Z) are the ground coordinates after correction, (X_{RF}, Y_{RF}, Z_{RF}) are ground coordinates derived from Equation 1 and the vender-provided RPCs, and (a_i, b_i, c_i) are correction coefficients.

Grodeki and Dial (2003) proposed a RPC block adjustment in image space for the accuracy improvement of the sensor models. They used denormalized RPC models, p and r, to express the object-space to image-space relationship, and the adjustable functions, Δp and Δr (which are added to the rational functions) to capture the discrepancies between the nominal and measured image space coordinates (Jacek, 2003).

The methods proposed by both Di *et al*. (2003) and Grodeki and Dial (2003) are polynomial models. Some are used in image domain, some in object domain. In general, these polynomial models can effectively correct the satellite sensor models and obtain a relative a good result. For example, after the sensor model refinement, Di *et al*. (2003) demonstrated a ground position accuracy of 1 to 2 meters for Ikonos images, and the experiment result of Grodeki and Dial (2003) also showed a ground position accuracy of 1 to 2 meters.

2.2.3 Refined sensor model for this research: In this research, a direct use of either of the above mentioned methods for sensor model refinement is not possible, because no ground

control points (GCPs) are available for the corrections or adjustments. To solve this problem, we utilize tie points identified in the Pan and MS images (i.e. roof corners, traffic marks on the surface of a road, etc.) to determine the corresponding GCPs on the ground (the general procedure will be described below). The ground GCPs are then applied to Equation 2 to find the corrections to the object ground coordinates derived from Equation 1 using the vender-provided RPCs. For refining the ground coordinates of a vehicle, these corrections are added into the vehicle ground coordinates derived from Equation 1 and the vender-provided RPCs. After this correction, the geometric accuracy of the vehicle coordinates is significantly improved. The refined coordinates of a vehicle from both the Pan and the MS images can then be used for the calculation of the speed and moving direction for achieving an acceptable speed calculation.

To derive ground GCPs from tie points selected in the Pan and MS images, the following procedure is applied:

(1) select k ($k \geq 4$) well-defined tie points (roof corners, traffic marks on the surface of a road, etc.) in both the Pan and MS images;
(2) calculate the ground coordinates of each tie point from Pan and MS images, respectively, using Equation 1 and the vender-provided RPCs, obtaining at least 4 sets of 3D ground coordinates for Pan, denoted as $(X_{RF}, Y_{RF}, Z_{RF})_{Pan,\,k}$ ($k \geq 4$), and 3D coordinates for MS, $(X_{RF}, Y_{RF}, Z_{RF})_{MS,\,k}$ ($k \geq 4$);
(3) average the coordinates $(X_{RF}, Y_{RF}, Z_{RF})_{Pan,\,k}$ and $(X_{RF}, Y_{RF}, Z_{RF})_{MS,\,k}$ from the same tie point to obtain an initially refined ground coordinates $(X, Y, Z)_k$' for the tie points;
(4) calculate the correction coefficients $(a_i, b_i, c_i)_{Pan}$ for the ground coordinates of the tie points in Pan image according to Equation 2 using corresponding $(X_{RF}, Y_{RF}, Z_{RF})_{Pan,\,k}$ and $(X, Y, Z)_k$', and calculate the correction coefficients $(a_i, b_i, c_i)_{MS}$ for the tie points in MS using corresponding $(X_{RF}, Y_{RF}, Z_{RF})_{MS,\,k}$ and $(X, Y, Z)_k$';
(5) apply $(a_i, b_i, c_i)_{Pan}$ and each of $(X_{RF}, Y_{RF}, Z_{RF})_{Pan,\,k}$ to Equation 2, respectively, to obtain refined ground coordinates of the tie points in Pan, $(X, Y, Z)_{Pan,\,k}$, and apply $(a_i, b_i, c_i)_{MS}$ and each of $(X_{RF}, Y_{RF}, Z_{RF})_{MS,\,k}$ to obtain refined ground coordinates of the tie points in MS, $(X, Y, Z)_{MS,\,k}$;
(6) average the $(X, Y, Z)_{Pan,\,k}$ and $(X, Y, Z)_{MS,\,k}$ of each tie point to obtain *k* further refined ground coordinates, $(X,Y, Z)_k$, with respect to both the Pan and MS images;
(7) use $(X, Y, Z)_{Pan,\,k}$ as $(X_{RF}, Y_{RF}, Z_{RF})_{Pan,\,k}$, $(X, Y, Z)_{MS,\,k}$ as $(X_{RF}, Y_{RF}, Z_{RF})_{MS,\,k}$, and $(X,Y, Z)_k$ as $(X, Y, Z)_k$' to repeat step (4), (5) and (6) until all the position differences between $(X,Y, Z)_k$ and those of the previous iteration are smaller than a threshold ε (e.g., 1% pixel); and
(8) accept the last coordinates $(X, Y, Z)_k$ as the GCPs derived from the *k* tie points.

Once the *k* GCPs are calculated from the *k* tie points, the GCPs are then employed to Equation 2 as the ground coordinates after correction (X, Y, Z) to determine the correction coefficients (a_i, b_i, c_i) using the ground coordinates (X_{RF}, Y_{RF}, Z_{RF}) derived from Equation 1 and the vender-provided RPCs. The correction coefficients (a_i, b_i, c_i) obtained from the tie points and the tie-point-derived GCPs can then be applied to the refinement of the ground coordinates of the vehicles from both the Pan and MS images.

2.3 Ground coordinates calculation

For many satellites, the geometric sensor models are given in the form of from ground coordinates to calculate image coordinates (Equation 1). That means, using a given ground coordinates (X, Y, H), we can calculate its image position using the sensor model. To calculate the ground positions of a vehicle from its image coordinates in Pan and MS images, however, the sensor model Equation 1 must be reversed. Hence, an iteration procedure needs to be performed, and the height information of the vehicle on ground needs to be obtained from a digital elevation model (DEM).

To simplify the calculation procedure, we first use the sensor model (Equation 1) to build a coarse linear transformation equation between image coordinates and ground coordinates, i.e., using (X, Y, 0) (assuming the high H = 0) to calculate its image coordinates (I, J) and then find a linear relationship between (X, Y) and (I, J), Equation 3:

$$X = f(I, J) \quad (3a)$$
$$Y = g(I, J) \quad (3b)$$
$$f(I, J) = a_1 I + b_1 J + c_1 \quad (3c)$$
$$g(I, J) = a_2 I + b_2 J + c_2 \quad (3d)$$

From Equation 3, with any image coordinates (I, J), we can obtain a coarse ground position (X, Y). From (X, Y), through DEM, we can get its height H. Then we use (X, Y, H) and the sensor model (1) to calculate its image coordinates (I', J'). From the two sets of image coordinates (I, J) and (I', J') we can get a image coordinate difference:

$$\Delta I = I - I' \quad (4a)$$
$$\Delta J = J - J' \quad (4b)$$

Then we use ΔI, ΔJ and (3) to correct its ground coordinates (X, Y), continue this procedure until ΔI, ΔJ are all smaller than a threshold, say 0.0001 pixel. The final (X, Y) is accepted as the ground coordinates of a vehicle.

3. EXPERIMENT

A set of level 1A (Basic) Quickbird imagery with the Pan, 0.61 meter, and MS, 2.44 meter, (figure 1) is tested with the developed technique. The imagery was acquired on July 26, 2002 over Gagetown, New Brunswick, Canada. The detailed data information of the subset is shown below.

MS Data:
Upper Left:
P (column): 2962 L (row): 5396
Lower Right
P (column): 3669 L (row): 6103

Pan Data:
Upper Left:
P (column): 11870 L (row): 20110
Lower Right
P (column): 14700 L (row): 22938

Because the Quickbird level 1A Pan and MS images are not registered, we firstly use 15 tie points to register the two

images together. Table 1 shows image coordinates both on MS and Pan images of the 15 tie points.

Because the coregistrated Pan and MS images need to be used to calculate the ground coordinates of vehicles from their image coordinates, the application of the refined sensor model Equation 1 and 2 as described in "Refined sensor model for this research" of section 2 is indispensable. Table 2 shows the relative positions of the 15 tie points deviation before sensor model refinement, and Table 3 shows the relative positions deviation after sensor model refinement.

These tables show that after sensor model refinement based on these tie points, the relative position mean deviation reduced from 3.47 meter to 1.33 meter (Figure 2).

Figure 3 and Table 4 shows the moving vehicles we selected on Pan image and MS image crossing the testing area (Figure 1). From the images below we can see many vehicles are very big. Normally we measured the vehicle's image coordinates at its central position. Then we use vehicle image coordinates to calculate its ground coordinates. From the two sets of ground coordinates calculated from the Pan and MS images and according to the time interval between Pan and MS, we can calculate vehicle's moving distance, moving speed and moving azimuth angle (Table 5).

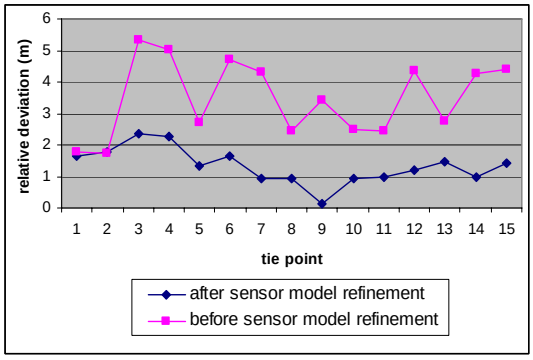

Figure 2. Position error before and after sensor model refinement

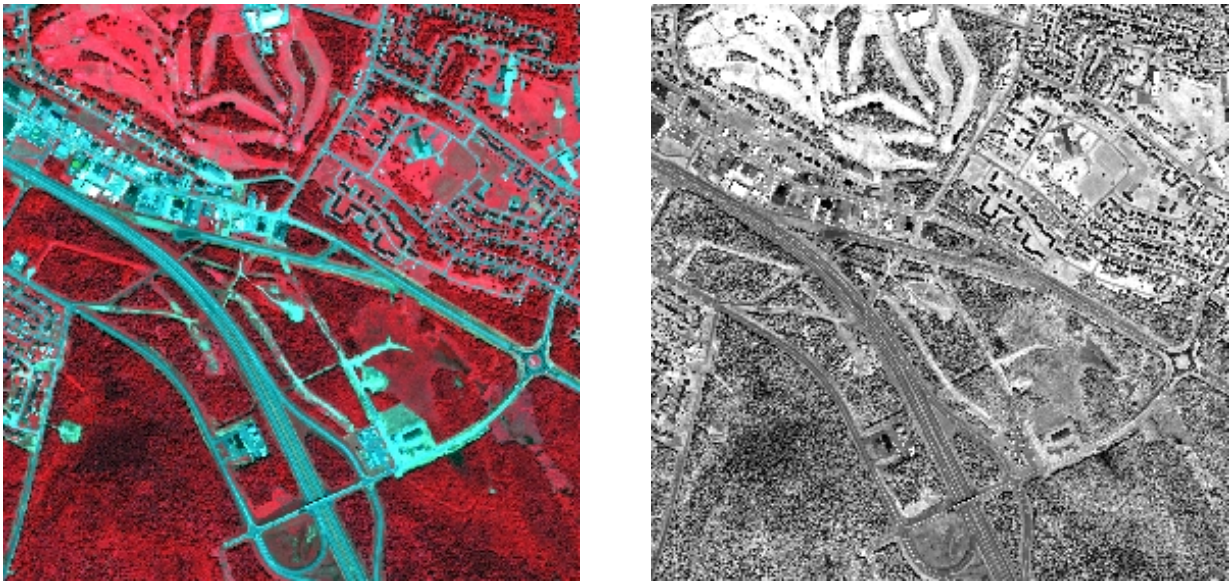

Figure 1. Quickbird MS (top) and Pan (bottom) images for moving vehicle detection (a subset of the testing area)

Table 2: Ground coordinates (WGS84) and relative deviation of tie points before sensor model refinement

No	X(m)	Y(m)	X(m)	Y(m)	Dev.(m)
1	694451.0	5079302.1	694449.7	5079302.4	1.7
2	700473.8	5079713.1	700472.6	5079712.5	1.7
3	694302.5	5076471.4	694298.9	5076470.2	5.3
4	700826.9	5077380.9	700823.7	5077382.7	5.0
5	697053.7	5076440.0	697052.0	5076441.4	2.6
6	698351.0	5079777.3	698347.8	5079776.3	4.7
7	693837.4	5079541.1	693834.4	5079540.9	4.3
8	693852.8	5079534.2	693851.0	5079534.1	2.4
9	693831.6	5079563.8	693829.2	5079563.7	3.4
10	693844.5	5079556.8	693842.7	5079556.7	2.4
11	693857.3	5079549.8	693855.6	5079549.7	2.4
12	693838.8	5079574.4	693835.9	5079573.6	4.3
13	693841.1	5079582.2	693839.3	5079583.4	2.7
14	693856.5	5079575.3	693853.5	5079575.8	4.2
15	693869.3	5079568.3	693866.3	5079569.5	4.3

Table 3: Ground coordinates (WGS84) and relative deviation of tie points after sensor model refinement

No	X(m)	Y(m)	X(m)	Y(m)	Dev.(m)
1	694449.9	5079301.6	694451.0	5079301.8	1.6
2	700472.0	5079712.6	700473.2	5079711.9	1.7
3	694301.4	5076470.8	694300.2	5076469.3	2.3
4	700825.4	5077380.2	700824.2	5077381.8	2.2
5	697052.4	5076439.4	697053.0	5076440.4	1.3
6	698349.5	5079776.8	698348.6	5079775.8	1.6
7	693836.4	5079540.6	693835.8	5079540.5	0.9
8	693851.8	5079533.7	693852.4	5079533.7	0.9
9	693830.6	5079563.4	693830.6	5079563.2	0.1
10	693843.5	5079556.3	693844.1	5079556.3	0.9
11	693856.3	5079549.3	693857.0	5079549.2	0.9
12	693837.9	5079574.0	693837.2	5079573.2	1.1
13	693840.1	5079581.8	693840.7	5079582.9	1.4
14	693855.5	5079574.9	693854.9	5079575.4	0.9
15	693868.3	5079567.9	693867.7	5079569.0	1.4

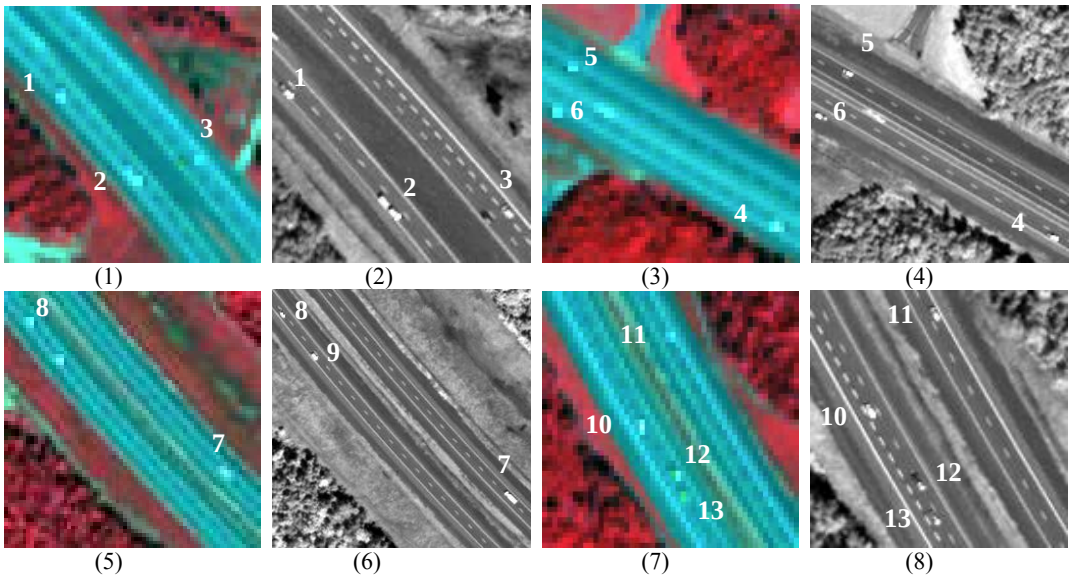

Figure 3. Moving vehicles in MS and Pan images for ground coordinates and moving speed calculation (each picture has different scale)

Table 4: Image coordinates of moving vehicles

NO	MS		Pan	
	P	L	P	L
1	331	706	1599	1531
2	345	723	1657	1597
3	358	719	1718	1596
4	166	583	939	1039
5	127	552	798	927
6	124	560	777	955
7	723	1362	3179	4172
8	670	1322	2955	3993
9	679	1332	2987	4034
10	608	1230	2707	3626
11	614	1212	2741	3576
12	615	1240	2733	3664
13	616	1244	2742	3682

Figure 4 shows the position, moving speed and moving direction of the vehicles. The arrow shows the moving direction. The longer this arrow is, the faster the vehicle moves.

From the table 5 and Figure 4, we can find that the mean speed is about 100 km/h. But some vehicles are moving very slow and some are very quick.

For example, the speed of vehicle 6 is only 23.8km/h and its moving direction is crossing road (Figure 4-(2)). The speed is very slow and the moving direction is not usual. However, from Figure 3-(4) and Figure 4-(2) we can see that vehicle 6 is on the road side, not in the drive lane. This speed should be reasonable. On the other hand, because there is still 1.33-meter relative position error after sensor model refinement, i.e. the calculated moving speed may have an error within 23.9 km/h, we guess this vehicle may just start up or slow down or stop there.

From Table 5 we can find that the vehicle 3 just has a speed of 68.15km/h. From Figure 3-(2) and Figure 4-(1) we can find, however, that vehicle 3 is in the slow lane just merging into the highway and there is a dark car close to it on the fast lane. Therefore, this speed is also reasonable for the situation.

From Table 5 we can also find some vehicles move very fast. Their speeds are over 140km/h. For example, vehicle 9 (Figure 3-(6) and Figure 4-(3)) is moving with speed 149km/h and vehicle 12 (Figure 3-(8) and Figure 4-(4)) at 145km/h. We can find that vehicle 9 is followed by vehicle 8 at a speed of just 113km/h. We guess vehicle 9 has just surpassed vehicle 8. For the same reason, vehicle 12 is passing vehicle 13 (figure 3-(8) and figure 4-(4)). Therefore, the speeds of vehicle 9 and 12 are also logic.

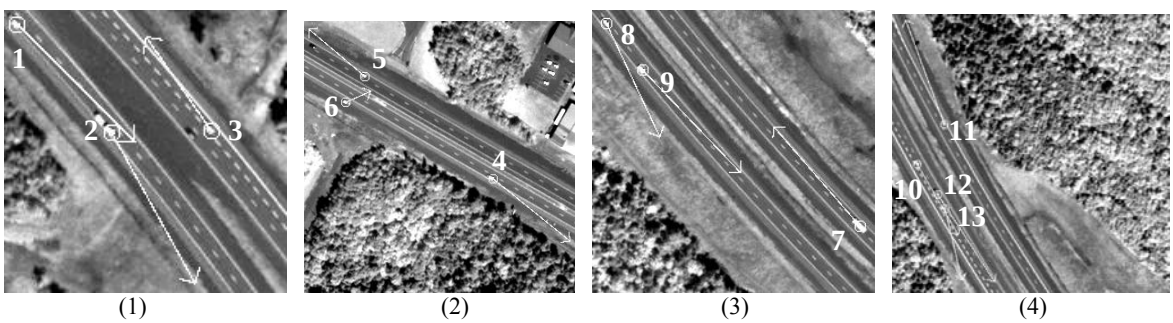

Figure 4. Moving speed and direction of individual vehicles (each picture has a different scale)

Table 5: Ground coordinates, speed, and azimuth angle of moving vehicles

No	X(m)	Y(m)	H(m)	Speed (km/h)	Azimuth (degree)
1	694447.8	5079066.2	29.5	118.5	133.8
2	694485.7	5079025.9	30.3	109.9	150.1
3	694524.2	5079028.5	30.5	68.1	323.1
4	694021.1	5079358.1	18.0	133.6	126.3
5	693929.8	5079424.8	15.4	93.1	306.8
6	693917.1	5079406.3	15.7	23.8	74.0
7	695493.5	5077424.5	30.5	135.7	317.7
8	695349.1	5077532.0	30.6	113.8	152.4
9	695370.0	5077506.8	30.6	149.7	134.3
10	695185.9	5077759.2	30.3	107.4	150.1
11	695206.4	5077792.3	30.2	145.6	337.5
12	695203.0	5077735.7	30.3	145.4	146.1

4. DISCUSSION

The accuracy of moving vehicle detection relies on the techniques of satellite sensor model refinement, image resolution, accuracy of vehicle image coordinates, accuracy of satellite time interval between Pan and MS, and DEM accuracy.

The accuracy of satellite time interval and image resolution is related to satellite equipment. We can consider them as constants. Because the time interval is very small, which means the intersection angle of Pan and MS is also very small, we can not calculate vehicle ground coordinates just based on its image coordinates on Pan and MS images. That means a DEM is necessary and the influence of DEM error to the ground coordinates calculation must be limited to a reasonable range.

In our current experiment, image coordinates of the vehicle centre, measured by mouse click, and is used for the speed calculation. The unit for image coordinates measurement is one pixel. That means a room for further improvement of measuring vehicle image coordinates still exist. The improvement of image coordinates measurement can further increase the accuracy of the moving speed calculation. Further research for the improvement of vehicle image coordinate measurement is ongoing.

5. CONCLUSION

A new technique for moving vehicle detection using a single set of high resolution satellite imagery is presented. The technique involves several steps including sensor model refinement, vehicle image coordinates measurement, and vehicle ground coordinates calculation. The experiment result shows that the technique can deliver moving vehicle's position, moving speed and moving direction effectively.

However, we recognized there is still big improvement potential in the vehicle image coordinates measurement. As the satellite time interval between Pan and MS is very small and vehicle's moving distance during the interval is very limited, even a very small improvement in the vehicle image coordinates measurement, such as 0.1 pixel, will significantly contribute to the accuracy improvement of moving speed calculation. Further research in this area is ongoing.

References

Defence R&D Canada, 2004, RADARSAT-2 Moving Object Detection Experiment (MODEX), Ottawa.

Di, K., R. Ma, and R. Li, 2003, Rational Functions and Potential for rigorous Sensor Model Recovery. *Photogrammetric Engineering & Remote Sensing*, Vol. 69, No. 1, pp. 33-41.

Dias, J. and P. Marques, 2005, Multiple Moving Target Detection and Trajectory Estimation Using a Single SAR Sensor. *IEEE Transactions on Aerospace and Electronic Systems*, Vol. 39, pp. 604–624.

Nag, S.; Barnes, M, 2003, A Moving Target Detection Filter for an Ultra-Wideband Radar. *Proceedings of the IEEE Radar Conference 2003*, 5-8 May 2003 Page(s): 147 – 153

Rad, R., and M. Jamzad, 2005, Real time classification and tracking of multiple vehicles in highways. *Pattern Recognition Letters*, Vol. 26, pp. 1597–1607.

STDI (Southwest Technology Development Institute) and U.S. Department of Transportation, 2000, A Summary of Vehicle Detection and Surveillance Technologies used in Intelligent Transportation Systems.

Sun, Z., G. Bebis, and R. Miller, 2005, On-Road Vehicle Detection Using Evolutionary Gabor Filter Optimization. *IEEE TRANSACTIONS ON INTELLIGENT TRANSPORTATION SYSTEMS,* VOL. 6, NO. 2, pp. 125-137.

Yamada, K. and M. Soga, 2003, A Compact Integrated Visual Motion Sensor for ITS Applications. *IEEE TRANSACTIONS ON INTELLIGENT TRANSPORTATION SYSTEMS*, VOL. 4, NO. 1, pp. 35-42.

Zhang, Y. and G. Hong, 2005, A wavelet integrated image fusion approach for target detection in very high resolution satellite imagery. *Proceedings of SPIE Defense and Security Symposium 2005*, Volumes 5806-5813, 28 Mar.–1 Apr. 2005, Orlando.